

A Solid–Gas Route to Polymorph Conversion in Crystalline $[\text{Fe}^{\text{II}}(\eta^5\text{-C}_5\text{H}_4\text{COOH})_2]$. A Diffraction and Solid-State NMR Study

Dario Braga, Fabrizia Grepioni,* and Marco Polito*

Dipartimento di Chimica G Ciamician, Università di Bologna, 40126 Bologna, Italy

Michele R. Chierotti, Silvano Ellena, and Roberto Gobetto*

Dipartimento di Chimica IFM, Università di Torino, 101256 Torino, Italy

Received May 29, 2006

Crystalline form I (monoclinic) and form II (triclinic) of ferrocene dicarboxylic acid $[\text{Fe}(\eta^5\text{-C}_5\text{H}_4\text{-COOH})_2]$ have been employed in solid–gas reactions at room temperature with the gaseous bases NH_3 , $\text{NH}_2(\text{CH}_3)$, and $\text{NH}(\text{CH}_3)_2$. The two crystal forms behave in exactly the same way in the solid–gas reaction, generating the same products, identified as the anhydrous crystalline salts $[\text{NH}_4]_2[\text{Fe}(\eta^5\text{-C}_5\text{H}_4\text{-COO})_2]$ (**1**), $[\text{NH}_3\text{CH}_3]_2[\text{Fe}(\eta^5\text{-C}_5\text{H}_4\text{COO})_2]$ (**2**), and $[\text{NH}_2(\text{CH}_3)_2]_2[\text{Fe}(\eta^5\text{-C}_5\text{H}_4\text{COO})_2]$ (**3**). Interestingly though, all these crystals revert via vapor release exclusively to the metastable crystalline form I. Starting materials and products have been investigated by single-crystal and powder diffraction and by ^{13}C , ^{15}N CPDAS and ^1H MAS methods.

Introduction

In previous papers we have shown that solvent-free reactions, such as those occurring between solid reactants or between a solid and a vapor,¹ provide viable routes, alternative to conventional reactions in solution, for the preparation of molecular salts and cocrystals. Reactions between molecular solids and between a molecular solid and a vapor have been the subject of investigations for more than a century in the field of organic–solid-state chemistry² and are still attracting considerable interest in the field of “green chemistry”,³ because these reactions do not require recovery, storage, and disposal of solvents.⁴ Solvent-free processes have now begun to be appreciated in the field of coordination and organometallic chemistry.⁵

In this paper we discuss the results of an investigation of reactivity toward volatile bases of different crystal forms of the sandwich organometallic dicarboxylic acid $[\text{Fe}(\eta^5\text{-C}_5\text{H}_4\text{COOH})_2]$.

$[\text{Fe}(\eta^5\text{-C}_5\text{H}_4\text{COOH})_2]$ has already proven to be a very useful reactant in the preparation of hybrid organic–organometallic and organometallic–organometallic crystal architectures by both solution and solid-state methods.^{6,7} For instance, it has been shown that crystalline $[\text{Fe}(\eta^5\text{-C}_5\text{H}_4\text{COOH})_2]$ reacts with vapors of 1,4-diazabicyclo[2.2.2]octane to quantitatively generate the corresponding organic–organometallic adduct $[\text{N}(\text{CH}_2\text{CH}_2)_3\text{-NH}][\text{Fe}(\eta^5\text{-C}_5\text{H}_4\text{COOH})(\eta^5\text{-C}_5\text{H}_4\text{COO})]$.⁸ The acid $[\text{Fe}(\eta^5\text{-C}_5\text{H}_4\text{-COOH})_2]$ also reacts in mechanochemical reactions with a number of solid bases.⁶

$[\text{Fe}(\eta^5\text{-C}_5\text{H}_4\text{COOH})_2]$ is known in three crystalline forms, a monoclinic form (form I), a triclinic form (form II), and a second triclinic form (form III). The hydrogen-bonded dimer $\{[\text{Fe}(\eta^5\text{-C}_5\text{H}_4\text{COOH})_2]\}_2$ is the fundamental supramolecular unit present in all forms, the major difference in the packing arrangement arising from the relative orientation of the hydrogen-bonded dicarboxylic dimers in the solid state. The structure of form III has been serendipitously determined and recently reported.⁹

Form I and form II can instead be obtained in a fairly straightforward manner (see below), which makes the dicarboxylic acid a good candidate for separate reactions with gases.

The aim of this work is threefold: (i) to investigate the behavior of different crystal forms of the same substance toward

* Corresponding authors. E-mail: fabrizia.grepioni@unibo.it.

(1) (a) Braga, D.; Grepioni, F. *Angew. Chem., Int. Ed.* **2004**, *43*, 2. (b) Braga, D.; Grepioni, F. *Chem. Commun.* **2005**, 29, 3635.

(2) (a) Pellizzari, G. *Gazz. Chim. Ital.* **1884**, *14*, 362. (b) Paul, I. C.; Curtin, D. Y. *Science* **1975**, *187*, 19. (c) Miller, R. S.; Curtin, D. Y.; Paul, I. C. *J. Am. Chem. Soc.* **1971**, *93*, 2784. (d) Miller, R. S.; Curtin, D. Y.; Paul, I. C. *J. Am. Chem. Soc.* **1972**, *94*, 5117. (e) Miller, R. S.; Curtin, D. Y.; Paul, I. C. *J. Am. Chem. Soc.* **1974**, *96*, 6329. (f) Chiang, C. C.; Lin, C.-T.; Wang, A. H.-J.; Curtin, D. Y.; Paul, I. C. *J. Am. Chem. Soc.* **1977**, *99*, 6303. (g) Miller, R. S.; Paul, I. C.; Curtin, D. Y. *J. Am. Chem. Soc.* **1974**, *96*, 6334. (h) Lin, C. T.; Paul, I. C.; Curtin, D. Y. *J. Am. Chem. Soc.* **1974**, *96*, 3699.

(3) Anastas, P. T.; Warner, J. C. *Green Chemistry: Theory and Practice*; Oxford University Press: New York, 1998.

(4) (a) Kaupp, G.; Kuse, A. *Mol. Cryst. Liq. Cryst.* **1998**, *313*, 36. (b) Kaupp, G. *Mol. Cryst. Liq. Cryst.* **1994**, *242*, 153. (c) Kaupp, G.; Schmeyer, J.; Haak, M.; Marquardt, T.; Herrmann, A. *Mol. Cryst. Liq. Cryst.* **1996**, *276*, 315. (d) Kaupp, G.; Schmeyer, J.; Boy, J. *Chem.–Eur. J.* **1998**, *4*, 2467. (e) Toda, F.; Takumi, H.; Akehi, M. *J. Chem. Soc., Chem. Commun.* **1990**, 1270. (f) Toda, F.; Okuda, K. *J. Chem. Soc., Chem. Commun.* **1991**, 1212. (g) Tanaka, K.; Fujimoto, D.; Oeser, T.; Irngartinger, H.; Toda, F. *Chem. Commun.* **2000**, 413. (h) Trask, A. V.; Jones, W. *Top. Curr. Chem.* **2005**, *254*, 41. (i) Kaupp G. *Top. Curr. Chem.* **2005**, *254*, 95. (j) Cave, G. W. V.; Raston, C. L.; Scott, J. L. *Chem. Commun.* **2001**, 2159. (k) Rothenberg, G.; Downie, A. P.; Raston, C. L.; Scott, J. L. *J. Am. Chem. Soc.* **2001**, *123*, 8701.

(5) (a) Braga, D.; Grepioni, F. *Top. Curr. Chem.* **2005**, *254*, 71. Applications to organometallic cases are less popular, see for example: (b) Albrecht, M.; Lutz, M.; Speck, A. L.; van Koten, G. *Nature* **2000**, *406*, 970. (c) Albrecht, M.; Gossage, R. A.; Lutz, M.; Speck, A. L.; van Koten, G. *Chemistry* **2000**, *6*, 1431. (d) Albrecht, M.; Schreurs, A. M. M.; Lutz, M.; Speck, A. L.; van Koten, G. *J. Chem. Soc., Dalton Trans.* **2000**, 3797. (e) Nichols, P. J.; Raston, C. L.; Steed, J. W. *Chem. Commun.* **2001**, 1062. (f) Belcher, W. J.; Longstaff, C. A.; Neckenig, M. R.; Steed, J. W. *Chem. Commun.* **2002**, 1602.

(6) Braga, D.; Maini, L.; Polito, M.; Mirolo, L.; Grepioni, F. *Chem.–Eur. J.* **2003**, *9*, 4362.

(7) Braga, D.; Maini, L.; Grepioni, F.; De Cian, A.; Felix, O.; Fischer, J.; Hosseini, M. W. *New J. Chem.* **2000**, *24*, 547.

(8) Braga, D.; Maini, L.; Polito, M.; Mirolo, L.; Grepioni, F. *Chem. Commun.* **2002**, 2960.

(9) Monoclinic form: (a) Palenik, G. J. *Inorg. Chem.* **1969**, *8*, 2744. Triclinic form: (b) Takusagawa, F.; Koetzle, T. F. *Acta Crystallogr., Sect. B* **1979**, *35*, 2888. Triclinic form: (c) Braga, D.; Polito, M.; D’Addario, D.; Grepioni, F. *Cryst. Growth Des.* **2004**, *1109*.

the same volatile reactant, (ii) to investigate the behavior of the same solid reactant toward different volatile bases, and (iii) to investigate whether the solid–gas reactions are reversible or, if this is not the case, which crystal form is adopted on desorbing the bases.

The first part of the project falls in the realm of crystal polymorphism. It has been argued and demonstrated that solid–vapor reactions can also be exploited for the preparation of polymorphic or solvate modifications of the same substance.¹⁰ Crystal polymorphism is a major scientific and industrial issue, because the same molecule in different crystal phases may possess different physical properties.¹¹

We therefore wondered if different crystal forms of $[\text{Fe}(\eta^5\text{-C}_5\text{H}_4\text{COOH})_2]$ would react in the same way in solid–gas reactions. While many groups are involved in studying how different crystalline forms of the same substance can be obtained, to the best of our knowledge the possibility of different chemical behavior of polymorphic modifications has been explored before only in the case of indomethacin amorphous and crystal forms reacted with ammonia by Stowell, Griesser, Byrn, et al.^{12a} and by us in the reaction of barbituric acid with volatile bases.^{12b}

To complement the information obtained by powder and single-crystal X-ray diffraction, we have made use of solid-state spectroscopic methods, which we have already applied to the investigation of a number of intriguing hydrogen-bonded crystalline materials. Nuclear magnetic resonance (NMR) spectroscopy is a potentially powerful tool for the investigation of the protonation states of molecules via ^1H , ^{13}C , and ^{15}N chemical shifts. This approach has been developed mainly for providing detailed insights into hydrogen-bonding interactions in the proteins.^{13–15}

Solid-state NMR can also find useful applications in the interpretation of the role of intermolecular bonding in the process of molecular recognition that leads to crystallization of organic molecules. Also in the case of weak interactions, diffraction techniques can be supported by NMR because of the marked sensitivity of NMR parameters of the nuclei (in particular hydrogen, carbon, and nitrogen) directly involved in chemical bonding.

Results and Discussion

The commercial crystalline powder of $[\text{Fe}(\eta^5\text{-C}_5\text{H}_4\text{COOH})_2]$ is mainly form I, as ascertained by X-ray powder diffraction

(10) (a) Braga, D.; Grepioni, F. *Chem. Soc. Rev.* **2004**, *4*, 229. (b) Braga, D.; Grepioni, F. In *Crystal Design, Structure and Function. Perspectives in Supramolecular Chemistry*, Desiraju, G. R., Whaley, J., Eds.; Chichester, UK, 2003; Vol. 7. Braga, D.; Grepioni, F. In *Static and Dynamic Structures of Organometallic Molecules and Crystals*; Brown, J. M., Hofmann, P., Eds.; *Topics in Organometallic Chemistry*, Vol. 4; Springer-Verlag: Berlin, Germany, 1999; p 48.

(11) (a) McCrone, W. C. In *Polymorphism in Physics and Chemistry of the Organic Solid State*; Fox, D., Labes, M. M., Weisseberger, A., Eds.; Interscience: New York, 1965; Vol. II, p 726. (b) Threlfall, T. L. *Analyst* **1995**, *120*, 2435. (c) Bernstein, J. *Polymorphism in Molecular Crystals*; Oxford University Press: Oxford, UK, 2002. (d) Braga, D. *Chem. Commun.* **2003**, 2751. (e) Dunitz, J.; Bernstein, J. *Acc. Chem. Res.* **1995**, *28*, 193. (f) Blagden, N.; Davey, R. J. *Cryst. Growth Des.* **2003**, *3*, 873. (g) Davey, R. J.; Allen, K.; Blagden, N.; Cross, W. I.; Lieberman, F. H.; Quayle, M. J.; Righini, S.; Seton, L.; Tiddy, G. J. T. *CrystEngComm* **2002**, *4*, 257. (h) Jetti, R. K. R.; Boese, R.; Sarma, J. A. R. P.; Reddy, L. S.; Vishweshwar, P.; Desiraju, G. R. *Angew. Chem., Int. Ed.* **2003**, *42*, 1963. (i) Bernstein, J.; *Chem. Commun.* **2005**, 5007.

(12) (a) Chen, X.; Morris, K. R.; Griesser, U. J.; Byrn, S. R.; Stowell, J. G. *J. Am. Chem. Soc.* **2002**, *124*, 15012. (b) Braga, D.; Cadoni, M.; Grepioni, F.; Maini, L.; K. Rubini *CrystEngComm* **2006**, in press.

(13) Wuthrich, K. *NMR in Biological Research: Peptides and Proteins*; North-Holland: Amsterdam, Holland, 1976.

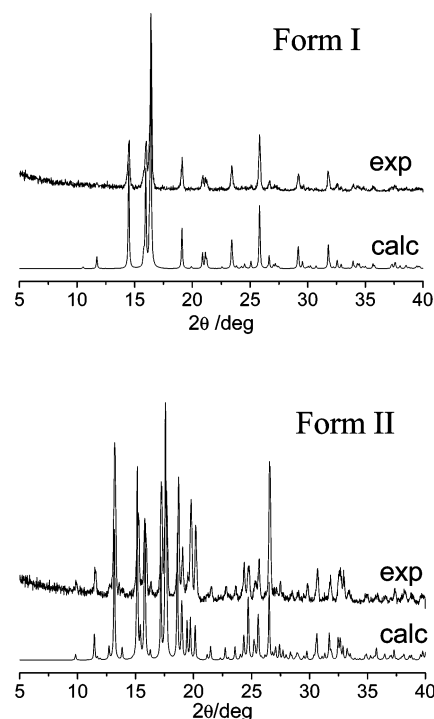


Figure 1. Comparison between the experimental powder diffraction patterns obtained for the two pure forms and those calculated on the basis of the known single-crystal structures of $[\text{Fe}(\eta^5\text{-C}_5\text{H}_4\text{-COH})_2]$.

(even though mixtures of forms I and II have been observed). The two forms are related by a monotropic thermodynamic relationship; that is, they do not interconvert at any given temperature before melting. However, since form II can be obtained from form I by the *slurry* method, form I is kinetically favored, albeit less thermodynamically stable than form II. Pure form II can be obtained by recrystallization from a room-temperature solution of form I in glacial acetic acid. Seeding has also been used to help precipitation of form II from the acetic acid solution.

Figure 1 shows a comparison between the experimental powder diffraction patterns obtained for the two pure forms and those calculated on the basis of the known single-crystal structures.

Uptake and Release of Ammonia from Forms I and II of $[\text{Fe}(\eta^5\text{-C}_5\text{H}_4\text{COOH})_2]$. Both form I and form II of $[\text{Fe}(\eta^5\text{-C}_5\text{H}_4\text{COOH})_2]$ react with vapors of aqueous ammonia (see Experimental Section) to give the same solid product, as characterized by X-ray powder diffraction. The experimental X-ray powder diffraction patterns are compared in Figure 2. It is evident that the two crystal forms lead to the same material.

Removal of NH_3 in a thermogravimetric experiment or by heating the powder product at $60\text{ }^\circ\text{C}$ under vacuum shows the loss of two moles of ammonia *per* ferrocenyl formula unit, which is in agreement with the formulation of **1** as $[\text{NH}_4]_2[\text{Fe}(\eta^5\text{-C}_5\text{H}_4\text{COO})_2]$. Ammonia removal from **1**, originating from either form I or form II, produces only the monoclinic form I, which is not the most thermodynamically stable of the two forms. This is not *per se* surprising, because there is no reason, if the reaction is quantitative, the crystalline salt product should “remember” which crystal form it comes from. It is instead of

(14) (a) Reynolds, W. F.; Peat, I. R.; Freedman, M. H.; Lyerla, J. R., Jr. *J. Am. Chem. Soc.* **1973**, *95*, 328. (b) Deslauriers, R.; McGregor, W. H.; Sarantakis, D.; Smith, I. C. P. *Biochemistry* **1974**, *13*, 3443.

(15) Harbison, G.; Herzfeld, J.; Griffin, R. G. *J. Am. Chem. Soc.* **1981**, *103*, 4752.

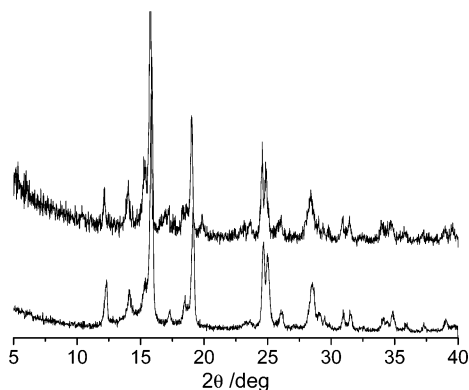


Figure 2. Comparison between the experimental powder diffractograms of compound **1**, obtained from the solid–gas reaction with ammonia of form I (top) and form II (bottom), respectively.

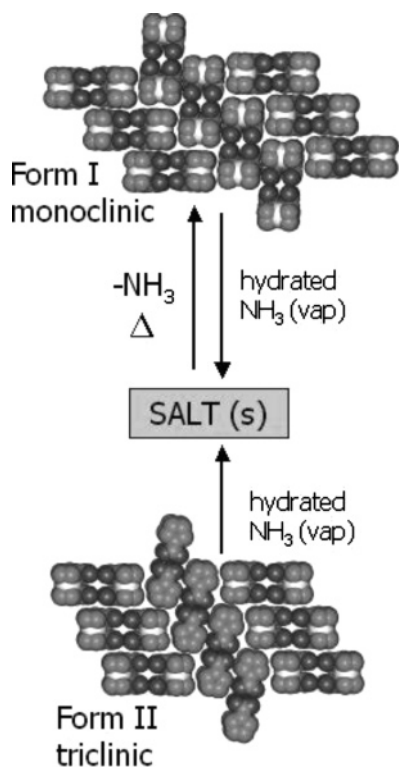


Figure 3. Reaction of crystalline forms I and II with vapors of NH_3 yielding the same salt, which upon heating and removal of NH_3 generates only the monoclinic form I.

relevance that forms I and II of $[\text{Fe}(\eta^5\text{-C}_5\text{H}_4\text{COOH})_2]$ are not known to interconvert via a solid–solid phase transition; hence they constitute a monotropic system: the ammonia absorption/release process, therefore, can be seen as a solid-state way to convert form II into form I. The process is schematically represented in Figure 3.

Reactions of Form I with NH_2CH_3 and with $\text{NH}(\text{CH}_3)_2$.

Once it had been established that forms I and II yield the same products with NH_3 , the following reactions with NH_2CH_3 and with $\text{NH}(\text{CH}_3)_2$ were carried out by using form I exclusively.

The reaction of $[\text{Fe}(\eta^5\text{-C}_5\text{H}_4\text{COOH})_2]$ with NH_2CH_3 proceeds quantitatively with formation of a single product, which has been analyzed by powder X-ray diffraction and solid-state NMR spectroscopy (see below). The powder pattern of product **2** shown in Figure 4 is very similar to the one observed in the case of NH_3 absorption. Similar consideration applies to the TGA of the desorption process, which indicates the loss of two

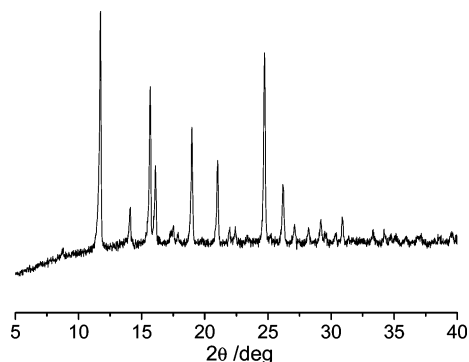


Figure 4. Powder X-ray diffractogram of compound **2**.

moles of reactant per formula unit. As in the case of **1**, we did not succeed in growing single crystals of **2** suitable for single-crystal diffraction experiments.

In the case of the solid–gas reaction with dimethylamine the formation of the product **3** could be confirmed by single-crystal X-ray diffraction. Figure 5 shows the packing arrangement of the dianion $[\text{Fe}(\eta^5\text{-C}_5\text{H}_4\text{COO})_2]^{2-}$ and of the cations $[\text{NH}_2(\text{CH}_3)_2]^+$. Anions and cations form a one-dimensional hydrogen-bonded network with $\text{N}^+\text{---H}\cdots\text{O}^-$ interactions between the oxygen atoms of the carboxylate groups and the two hydrogen atoms on the dimethylammonium cation [$\text{N}\cdots\text{O}$ 2.680(5) and 2.722(5) Å]. A comparison between the measured X-ray diffraction pattern and the one calculated on the basis of the single-crystal structure is shown in Figure 6.

As in the previous cases, desorption of the base leads to quantitative conversion back to form I. On the basis of the similarity between the powder diffractograms and the TGAs of compounds **1**, **2**, and **3**, and in view of the same behavior toward absorption and release one can expect the three compounds to possess very similar crystal structures.

It is worth recalling here that the reaction carried out in solution with $\text{NH}(\text{CH}_3)_2$ by Glidewell et al.¹⁶ yielded the mono-deprotonated anhydrous salt of formula $[\text{NH}_2(\text{CH}_3)_2]^+[\text{Fe}(\eta^5\text{-C}_5\text{H}_4\text{COOH})(\eta^5\text{-C}_5\text{H}_4\text{COO})]^-$. The structure of this compound was shown to be composed of chains of monoanions hydrogen bonded via COOH/COO^- groups, with the dimethylammonium cations between the chains.

NMR Spectroscopy. The ^{13}C spectra (Figure 7, A and B) of monoclinic and triclinic $\text{Fe}(\eta^5\text{-C}_5\text{H}_4\text{COOH})_2$ recorded at high spinning speeds show different features in the carboxylic region. Indeed the spectrum of form I presents a single resonance at 176.2 ppm for the COOH group, while the spectrum of form II shows two close peaks at 177.4 and 175.9 ppm. Furthermore only a small but significant difference in the position of the Cp carbons located at 74.3 ppm (triclinic form) and at 74.0 ppm (monoclinic form) is observed. These clear differences are in agreement with the different packing arrangements of the two crystal forms observed by X-ray;⁹ the presence of a single molecule in the asymmetric unit for form I and of two independent molecules for form II. In form I the geometries of the COOH groups of the single molecule are almost equivalent (C–O distances: 1.254, 1.274 Å and 1.264, 1.276 Å), suggesting that the proton lies close to the middle point of the hydrogen bond (HB), as already observed in similar compounds.¹⁷ On the contrary, in form II the constraint by symmetry leads to a small but significant difference in the two molecules (C–O

(16) Zakaria, C. M.; Ferguson, G.; Lough, A. J.; Glidewell, C. *Acta Crystallogr., Sect. B* **2002**, *58*, 786.

(17) Braga, D.; Maini, L.; Giuffreda, S. L.; Grepioni, F.; Chierotti, M. R.; Gobetto, R. *Chem.–Eur. J.* **2004**, *10*, 3261.

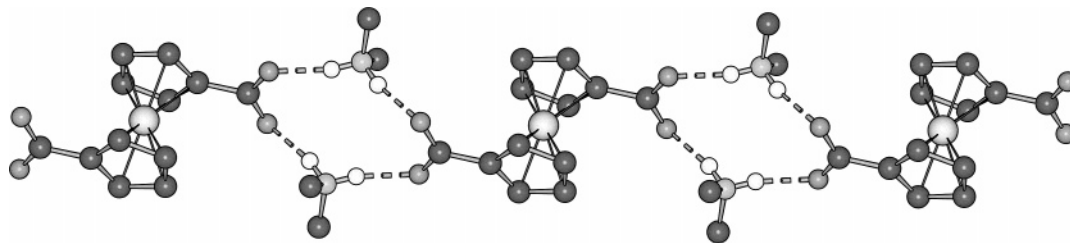


Figure 5. Packing arrangement of the dianion $[\text{Fe}(\eta^5\text{-C}_5\text{H}_4\text{COO})_2]^{2-}$ and of the cations $[\text{NH}_2(\text{CH}_3)_2]^+$ showing the $\text{N}^+-\text{H}\cdots\text{O}^-$ interactions between the oxygen atoms of the carboxylate groups and the two hydrogen atoms on the dimethylammonium cation.

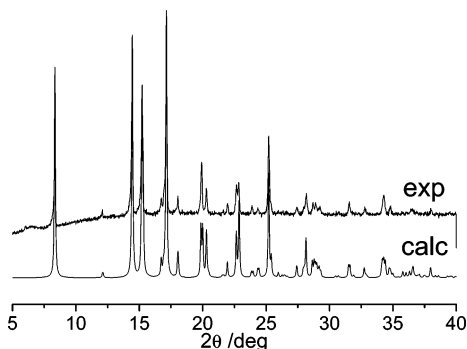


Figure 6. Comparison between the measured X-ray diffraction pattern and the one calculated on the basis of the crystal structure of compound 3.

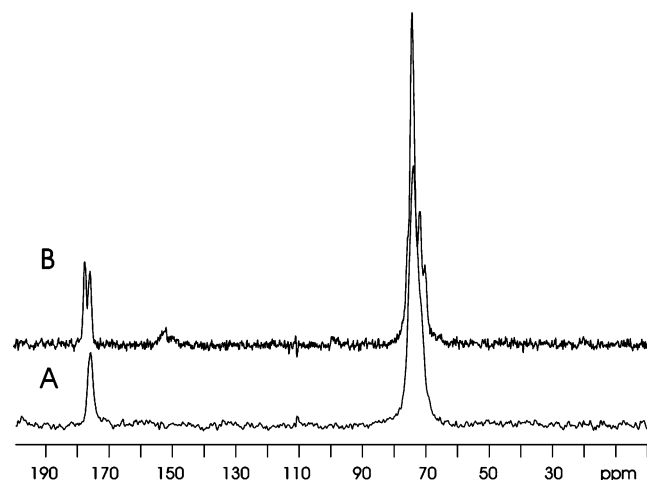


Figure 7. ^{13}C CPMAS spectra of monoclinic $[\text{Fe}(\eta^5\text{-C}_5\text{H}_4\text{COOH})_2]$ (form I) (A) and triclinic $[\text{Fe}(\eta^5\text{-C}_5\text{H}_4\text{COOH})_2]$ (form II) (B) recorded at 67.9 MHz, at the spinning speed of 5.5 kHz.

distance in molecule 1: 1.230, 1.308 Å and 1.230, 1.302 Å; C–O distance in molecule 2: 1.239, 1.294 Å and 1.234, 1.395 Å). In the triclinic form this difference is reflected in a difference in the acidity of the carboxylic groups; in fact, in molecule 2, the hydrogen-bonded protons are no longer in the middle of the interaction, but they are closer to a specific carboxylate group. Therefore it is now possible to distinguish a COOH group with a more pronounced carboxylic character (that resonates at 175.9 ppm in molecule 1) and one with a more pronounced carboxylate character (that resonates at 177.4 ppm in molecule 2). Accurate analysis of the carboxylic sideband pattern for a series of spectra recorded at different spinning rates affords the chemical shift tensor values reported in Table 1. Of course the difference between the two groups is small; however they are in agreement with previously reported data, where the δ_{11} value increases on passing from carboxylate to carboxylic acid form, δ_{22} shows an opposite variation, while changes in δ_{33} do not

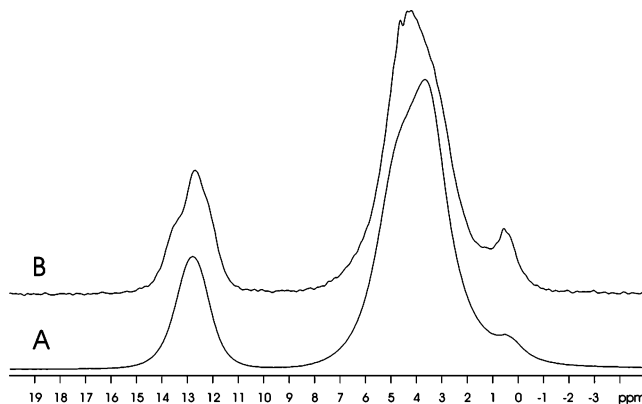


Figure 8. ^1H MAS spectra of monoclinic $\text{Fe}(\eta^5\text{-C}_5\text{H}_4\text{COOH})_2$ (form I) (A) and triclinic $\text{Fe}(\eta^5\text{-C}_5\text{H}_4\text{COOH})_2$ (form II) (B) recorded at 600 MHz, at the spinning speed of 35 kHz.

Table 1. ^{13}C Isotropic Chemical Shifts and Chemical Shift Tensors (δ_{11} , δ_{22} , δ_{33}) for Monoclinic and Triclinic $[\text{Fe}(\eta^5\text{-C}_5\text{H}_4\text{COOH})_2]$

compound	δ_{iso}	δ_{11}	δ_{22}	δ_{33}
$[\text{Fe}(\eta^5\text{-C}_5\text{H}_4\text{COOH})_2]$ triclinic	177.4	234.7	190.5	107.0
	175.9	227.9	198.6	101.1
	74.3	132.0	71.3	19.5
$[\text{Fe}(\eta^5\text{-C}_5\text{H}_4\text{COOH})_2]$ monoclinic	176.2	228.4	192.0	108.4
	74.0	126.2	76.8	19.1

seem to be correlated with the carboxylic or carboxylate character of the group.¹⁸

The ^1H MAS spectra of the two polymorphs do not show significant differences (Figure 8): they are characterized by two signals at about 12.7 ppm and at 3.7–4.1 ppm assigned to the hydrogen-bonded protons and to the Cp protons, respectively. This is not surprising if one considers that the hydrogen-bonded proton chemical shift is influenced by the X–H bond polarization. In other words, it relates more to the strength of the interaction than to the position of hydrogen.¹⁹ That means that despite the different position of the proton along the hydrogen bond in form I and form II, the strength of the interactions is similar, as confirmed also by the O–O distances (form I: 2.635, 2.593 Å; form II: molecule 1 2.672, 2.626 Å and molecule 2 2.621, 2.643 Å). The spectra differ only in a shoulder observed at about 13.4 ppm in the spectrum of form II. It is interesting, instead, to compare the relaxation data obtained by measuring the ^1H T_1 . In fact form I exhibits short longitudinal relaxation times of 326 and 467 ms for the peaks at 3.7 and 12.7 ppm, respectively, while form II shows a T_1 value more than 2 orders of magnitude greater than that of form I. Indeed for the signal at 4.4 ppm it is about 143 s, while for the resonance at 12.7 ppm it is 137 s. The T_1 values of the two polymorphs can be

(18) Braga, D.; Maini, L.; de Sanctis, G.; Grepioni, F.; Chierotti, M. R.; Gobetto, R. *Chem.-Eur. J.* **2003**, *9*, 5538.

(19) Sternberg, U.; Brunner, E. *J. Magn. Reson. A* **1994**, *108*, 142.

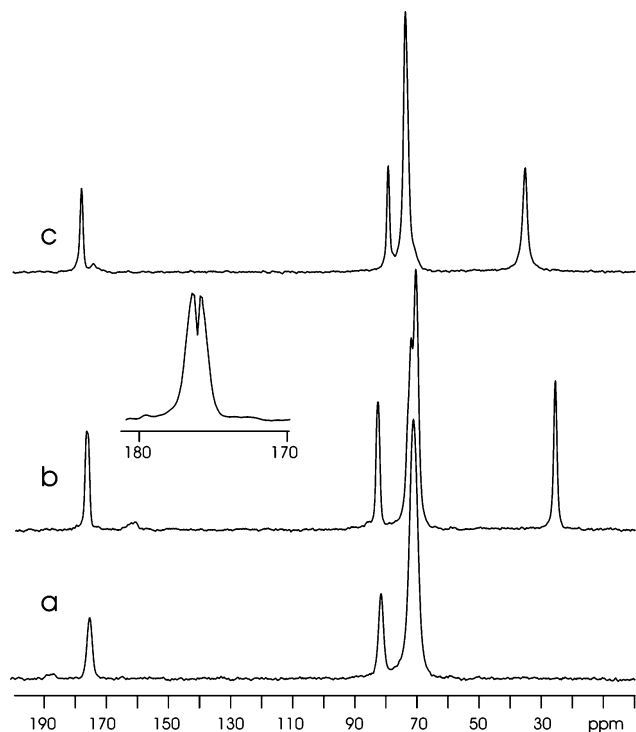


Figure 9. ^{13}C CPMAS spectrum of **1** (a), **2** (b), and **3** (c) recorded at 67.9 MHz, at the spinning speed of 5.5 kHz.

explained by the presence of a different mobility or by the different efficiency of the dipolar relaxation mechanism.

The ^{13}C spectra of the products obtained by solid–gas reaction of crystalline forms I and II with NH_3 , NH_2CH_3 , and $\text{NH}(\text{CH}_3)_2$ have been recorded in order to establish whether different structures can be revealed by solid-state NMR techniques. This hypothesis is based on the fact that accurate information can be obtained by solid-state NMR in samples that are lacking order as a result of the solid–gas reaction.

In Figure 9a–c the ^{13}C CPMAS NMR spectra are reported. The observation of different isotropic chemical shifts for the carboxylic groups and, overall, for the Cp moieties with respect to the free ferrocene molecule confirms that the reaction took place in all cases. Although spectra 10a, b, and c are different, the shifts observed are small and it is reasonable to propose that hydrogen bonding and crystal packing are similar. Probably the main differences stem only from the energy and the strength of the interactions that constitute the supramolecular network.

The ^{13}C spectrum of **1** is characterized by a peak at δ 175.5 for the COOH, while the Cp signal is split into two resonances centered at 81.7 and 71.2 ppm for the quaternary carbon C1 and for the other four carbon atoms, respectively (Figure 9a).

In the carboxylic region of the spectrum of compound **2** (Figure 9b) two signals are present at δ 176.5 and 175.7. In the low-frequency region three peaks are observed at 82.6, 71.8, and at 70.4 ppm for the Cp carbon atoms, while a fourth resonance at 25.4 ppm is attributed to the amine methyl group. The two carboxylic peaks can be explained with the presence of different phases or, alternatively, with crystallographically different COOH groups.

The spectrum of compound **3** (Figure 9c) shows the greatest shift for the carboxylic peak from δ 176.2 to δ 178.0. According

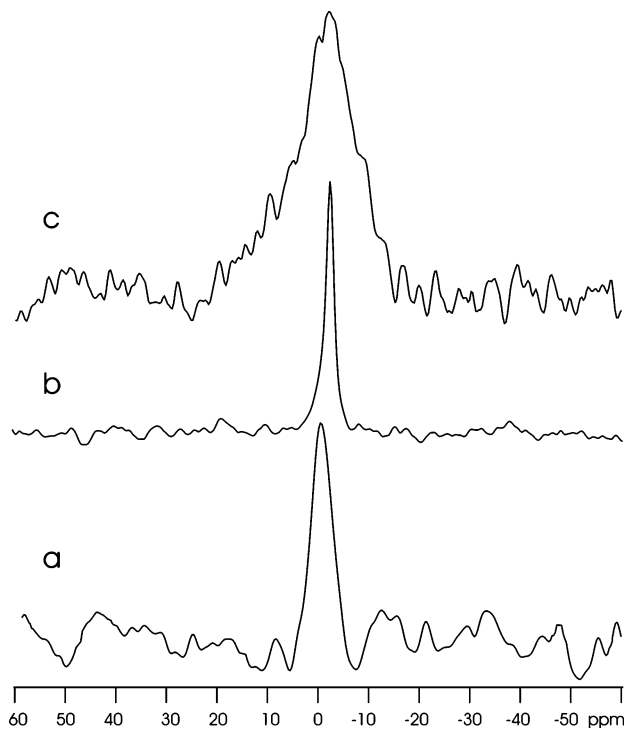


Figure 10. ^{15}N CPMAS spectrum of **1** (a), **2** (b), and **3** (c) recorded at 27.25 MHz, at the spinning speed of 4.0 kHz.

Table 2. ^{13}C and ^{15}N NMR Data for Compounds 1–3

compound	^{13}C δ_{iso}	^{15}N δ_{iso}
[NH_4] $_2$ [Fe(η^5 -C $_5$ H $_4$ COO) $_2$] (1)	175.5	−0.5
	81.7	
	71.2	
[NH_3CH_3] $_2$ [Fe(η^5 -C $_5$ H $_4$ COO) $_2$] (2)	176.5	−2.3
	175.7	
	82.6	
	71.8	
[$\text{NH}_2(\text{CH}_3)_2$] $_2$ [Fe(η^5 -C $_5$ H $_4$ COO) $_2$] (3)	70.4	−2.0
	25.4	
	178.0	
	79.3	
	73.8	
	35.2	

to the literature,²¹ this indicates a more pronounced carboxylate character for the COOH group of **3** with respect to the others. The signals of the Cp moiety are observed at 79.3 and 73.8 ppm, while the methyl group gives rise to a single resonance at 35.2 ppm.

The ^{15}N CPMAS for the three compounds **1**, **2**, and **3** (Figure 10a–c) are characterized by a single resonance in the range 0.0 to −3.0 ppm. From the literature²¹ this chemical shift is typical of a NH_4^+ group, in agreement with the presence of a protonated amine, as observed by X-ray crystallography in compound **3**. ^{15}N chemical shifts are reported in Table 2. The chemical shift changes detected for the products are probably due to the variation in strength or in length of the hydrogen bond interaction determined by the different acceptor capability of the base having H, CH_3 , or $(\text{CH}_3)_2$ substituents. The broad peak observed in the ^{15}N spectrum of **3** (Figure 10c) suggests the presence of disorder in the hydrogen bond network.

(20) (a) Naito, A.; Ganapathy, S.; Akasaka, K.; McDowell, C. J. *J. Chem. Phys.* **1981**, *74*, 3198. (b) Haberkorn, R.; Stark, R.; van Willigen, H.; Griffin, R. *J. Am. Chem. Soc.* **1981**, *103*, 2534. (c) James, N.; Ganapathy, S.; Oldfield, E. *J. Magn. Reson.* **1983**, *54*, 111. (d) Griffin, R.; Pines, A.; Pausak, S.; Waugh, J. *J. Phys. Chem.* **1975**, *65*, 1267.

(21) (a) Levy, G. C.; Lichter, R. L. *Nitrogen-15 Nuclear Magnetic Resonance Spectroscopy*; John Wiley & Sons: New York, 1979. (b) Litchmann, W. M.; Alei, M., Jr.; Florin, A. E. *J. Am. Chem. Soc.* **1970**, *92*, 4828. (c) Duthaler, R. O.; Roberts, J. D. *J. Magn. Reson.* **1979**, *34*, 129.

Experimental Section

General Comments. The commercial crystalline powder of $[\text{Fe}(\eta^5\text{-C}_5\text{H}_4\text{COOH})_2]$ from Fluka (form I) was used without any further purification. The triclinic form was obtained by slow evaporation of a solution of $[\text{Fe}(\eta^5\text{-C}_5\text{H}_4\text{COOH})_2]$ in acetic acid.

Reaction of $[\text{Fe}(\eta^5\text{-C}_5\text{H}_4\text{COOH})_2]$ Form I and II with NH_3 . Exposure of a finely ground crystalline powder of $[\text{Fe}(\eta^5\text{-C}_5\text{H}_4\text{COOH})_2]$ (200 mg) to the vapors of NH_3 was attained by allowing the vapors of a 30% aqueous solution (10 mL) contained in a round-bottom flask to pass into a filter funnel, in which a glass sample holder containing the crystalline complex was placed. In this way the powder and the solution were not in contact; the reaction took place in a closed system. The reaction is complete after 10 min. No difference was noted in the rate of the gas uptake process between form I and form II.

Elemental analysis for compound **1** (as obtained from the reaction of form I with NH_3), $\text{C}_{12}\text{H}_{16}\text{N}_2\text{O}_4\text{Fe}$: calcd C 46.78, H 5.23, N 9.09; found C 46.87, H 5.24, N 9.06.

Reaction of $[\text{Fe}(\eta^5\text{-C}_5\text{H}_4\text{COOH})_2]$ Form I with NH_2CH_3 and $\text{NH}(\text{CH}_3)_2$. Exposure of a finely ground crystalline powder of $[\text{Fe}(\eta^5\text{-C}_5\text{H}_4\text{COOH})_2]$ (200 mg) to the vapors of a 30% aqueous solution NH_2CH_3 or $\text{NH}(\text{CH}_3)_2$ was attained by allowing the vapors of the corresponding solutions (10 mL) contained in a round-bottom flask to pass into a filter funnel, in which a glass sample holder containing the crystalline complexes was placed. In this way the powder and the solution were not in contact; the reaction took place in a closed system. The reaction is complete after 10 min.

Elemental analysis for compound **2**, $\text{C}_{14}\text{H}_{20}\text{N}_2\text{O}_4\text{Fe}$: calcd C 50.02, H 6.00, N 8.33; found C 49.87, H 6.01, N 8.27. Elemental analysis for compound **3**, $\text{C}_{16}\text{H}_{24}\text{N}_2\text{O}_4\text{Fe}$: calcd C 52.76, H 6.64, N 7.69; found C 52.65, H 6.63, N 7.67.

Crystal Structure Determination of **3.** Crystal data were collected on a Bruker ApexII CCD diffractometer. Mo $K\alpha$ radiation, $\lambda = 0.71073$ Å, monochromator graphite. $\text{C}_{16}\text{H}_{24}\text{FeN}_2\text{O}_4$, $M_r = 364.22$, orange crystals; monoclinic $C2/c$, $a = 21.474(4)$ Å, $b = 7.771(1)$ Å, $c = 10.485(1)$ Å, $\beta = 99.453(4)^\circ$, $V = 1725.9(4)$ Å³, $Z = 4$, $D_{\text{calc}} = 1.402$ g cm⁻³, $R1$ ($wR2$) 0.0520 (0.1258) for 1526 observed independent reflections; 2θ range = $6.0\text{--}50.0^\circ$. *SHELX97*^{2a} was used for structure solution and refinement based on F^2 . Non-hydrogen atoms were refined anisotropically. Hydrogen atoms bound to carbon atoms and to the nitrogen atom of the cation were added in calculated positions and refined. *SCHAKAL99*^{22b} was used for the graphical representation of the results. The program *PLATON*^{22c} was used to calculate hydrogen-bonding interactions. Powder data were collected on a Philips X'Pert automated diffractometer with Cu $K\alpha$ radiation, graphite monochromator. The program *PowderCell 2.2*^{23d} was used for calculation of X-ray powder patterns.

NMR Spectroscopy. All ¹³C and ¹⁵N NMR spectra were obtained by using a JEOL GSE 270 (6.34 T) spectrometer operating at 67.9 MHz for ¹³C and at 27.25 MHz for ¹⁵N, equipped with a Doty XC5 probe. The ¹³C spectra were recorded at a spinning rate in the range from 5 to 6 kHz under conditions of ¹H–¹³C cross-polarization, high-power proton decoupling, and magic angle spinning. The 90° pulse was 4.5 μs, and the contact pulse was 3.5 ms. The spectra were collected after 1500 scans using a recycle delay of 10 s. The line broadening was set to be 10 Hz. The ¹⁵N CPMAS spectra were recorded at a spinning rate of about 4 kHz. A contact time of 5 ms, a repetition time of 10 s, and a spectral width of 35 kHz were used for accumulation of 3600 transients. The fid's were processed with a line broadening of 25 Hz. Cylindrical 5 mm o.d. zirconium rotors with a sample volume of 120 μL were employed. For all samples the magic angle was carefully adjusted from the ⁷⁹Br MAS spectrum of KBr by minimizing the line width of the spinning sideband satellite transitions. The ¹³C chemical shifts were referred to external hexamethylbenzene, setting the methyl carbon to 17.4 ppm down-

field from tetramethylsilane (TMS), while the ¹⁵N chemical shifts were referenced via the resonance of solid $(\text{NH}_4)_2\text{SO}_4$ (-355.8 ppm with respect to CH_3NO_2).

The principal components of the chemical shift tensors were extracted by computer simulation (HBA-graphical)²³ of the spinning sideband patterns obtained at low speed using the algorithm developed by Herzfeld and Berger.²⁴ The errors in the evaluation of the chemical shift tensor were estimated to be less than 4 ppm by repeating the calculation at different spinning speeds. The chemical shift tensors were reported following the standard convention where $\delta_{11} > \delta_{22} > \delta_{33}$, $\delta_{\text{iso}} = (\delta_{11} + \delta_{22} + \delta_{33})/3$ and $\Delta\delta = \delta_{33} - (\delta_{11} + \delta_{22})/2$.

¹H MAS spectra were recorded on a Bruker AVANCE600WB with a double resonance 2.5 mm probe spectrometer operating at 600 MHz for ¹H. Powdered samples were spun at about 30–35 kHz. Spectra were acquired using an Eyring pulse sequence in order to prevent the baseline from rolling due to the acoustic ringing of the probehead and in order to delete the proton signal background. A $\pi/2$ pulse of 2.4 μs in duration and a pulse delay of 1 s over a spectral width of 100 kHz were used. A total of 16 transients were collected for each spectrum. Proton chemical shifts were referenced via the resonance of PDMSO (polydimethylsiloxane) at 0.14 ppm relative to TMS.

T₁ Measurements. Spin–lattice relaxation times in MAS mode were measured by the inversion recovery pulse sequence.

Conclusions

In this paper we have reported on the investigation of a series of solid–gas reactions between polycrystalline samples of the organometallic acid $[\text{Fe}(\eta^5\text{-C}_5\text{H}_4\text{COOH})_2]$, as its monoclinic and triclinic polymorphic forms, and the gaseous bases NH_3 , $\text{NH}_2\text{-}(\text{CH}_3)$, and $\text{NH}(\text{CH}_3)_2$.

High-resolution ¹³C-CPMAS spectra and proton relaxation data reveal substantial differences between monoclinic and triclinic forms of $[\text{Fe}(\eta^5\text{-C}_5\text{H}_4\text{COOH})_2]$.

In all cases it has been possible to ascertain rapid reaction between the acid and the bases with formation of the corresponding polycrystalline salts $[\text{NH}_4]_2[\text{Fe}(\eta^5\text{-C}_5\text{H}_4\text{COO})_2]$ (**1**), $[\text{NH}_3\text{CH}_3]_2[\text{Fe}(\eta^5\text{-C}_5\text{H}_4\text{COO})_2]$ (**2**), and $[\text{NH}_2(\text{CH}_3)_2]_2[\text{Fe}(\eta^5\text{-C}_5\text{H}_4\text{COO})_2]$ (**3**). The structures of these salts are very similar on the basis of a comparison of powder diffractograms and NMR spectra, which also helped in assigning the chemical formulas to compounds **1** and **2**, for which no single crystals could be obtained. In the case of **3** the structure has been ascertained by a single-crystal X-ray diffraction experiment showing that the structure is the same as that of the bulk product. TGA and variable-temperature X-ray powder diffraction experiments have been used to investigate the reversibility of the processes and the nature of the products. It has been shown that, while in all cases the uptake of gas is a reversible process, the loss of gas invariably leads to form I of $[\text{Fe}(\eta^5\text{-C}_5\text{H}_4\text{COOH})_2]$; therefore the acid–base reaction is reversible only when it involves form I as the organometallic starting material, while the reaction of form II with vapors of ammonia is not reversible. It is worth pointing out that the absorption/desorption processes imply profound and dramatic structural rearrangements. For example,

(22) (a) Sheldrick, G. M. *SHELX-97*, Program for Crystal Structure Determination; University of Göttingen: Göttingen, Germany, 1997. (b) Keller, E. *SCHAKAL99*, Graphical Representation of Molecular Models; University of Freiburg: Freiburg, Germany, 1999. (c) Spek, A. L. *PLATON. Acta Crystallogr., Sect. A* **1990**, *46*, C31. (d) *PowderCell* program by Kraus, W.; Nolze, G. (BAM Berlin) subgroups derived by Ulrich Müller (Gh Kassel).

(23) Eichele, K.; Wasylishen, R. E. *HBA* ver. 1.5, Program for Herzfeld-Berger Analysis; Dalhousie University: Halifax, Canada, 2005.

(24) Herzfeld, J.; Berger, A. E. *Chem. Phys.* **1980**, *73*, 6021.

the ferrocenyl moiety has to change from an eclipsed *cisoid* conformation of the substituted cyclopentadienyl rings to a staggered *transoid* conformation on passing from the crystalline acid to the salt and vice versa. The conformational change is also accompanied by the proton transfer processes detected by solid-state NMR: from the neutral acid to the incoming neutral molecules of the bases and from these to the carboxylate groups, with re-formation of the carboxylic acid cyclic structure, when the bases are thermally removed. One may envisage a mechanism of phase reconstruction upon reaction of the type described by Kaupp.⁴ It can be argued that these reactions are not bona fide solid–gas solvent-free processes because water vapor may act as a lubricant or “temporary solvent” during the uptake process and formation of the salts. This argument holds true for the uptake process but cannot be applied to the reverse process, where vapors are desorbed.

Finally, we have shown that gas desorption from **1**, **2**, and **3** leads exclusively to form I, thus representing an effective way to convert form II into form I via salt formation. Since the

controlled preparation and characterization of crystal polymorphs is a major issue of modern crystal engineering and solid-state chemistry, the observation that the transformation of the most stable form II into the less stable form I of otherwise non-interconverting polymorphs can be obtained in a solvent-free reaction via the intermediacy of salt formation is of some interest.

Acknowledgment. We thank MIUR (PRIN 2004 and FIRB2001) and the Universities of Bologna and Torino for financial support. We thank Hans Foester (Bruker Biospin, Karlsruhe, Germany) for recording the 600 MHz proton spectra and the ¹H *T*₁ measurements.

Supporting Information Available: ORTEP diagram, tables of coordinates, bond lengths and angles, and anisotropic displacement parameters for **3**. This material is available free of charge via the Internet at <http://pubs.acs.org>.

OM060468W